Simultaneous Trajectory Planning and Tracking Using an MPC Method for Cyber-Physical Systems: A Case Study of Obstacle Avoidance for an Intelligent Vehicle

Hongyan Guo, *Member, IEEE*, Chen Shen, Hui Zhang, *Senior Member, IEEE*, Hong Chen, *Senior Member, IEEE*, and Rui Jia

***Abstract*—As a typical example of cyber-physical systems, intelligent vehicles are receiving increasing attention, and the obstacle avoidance problem for such vehicles has become a hot topic of discussion. This paper presents a simultaneous trajectory planning and tracking controller for use under cruise conditions based on a model predictive control (MPC) approach to address obstacle avoidance for an intelligent vehicle. The reference trajectory is parameterized as a cubic function in time and is determined by the lateral position and velocity of the intelligent vehicle and the velocity and yaw angle of the obstacle vehicle at the start point of the lane change maneuver. Then, the control sequence for the vehicle is incorporated into the expression for the reference trajectory that is used in the MPC optimization problem by treating the lateral velocity of the intelligent vehicle at the end point of the lane change as an intermediate variable. In this way, trajectory planning and tracking are both captured in a single MPC optimization problem. To evaluate the effectiveness of the proposed simultaneous trajectory planning and tracking approach, joint veDYNA-Simulink simulations were conducted in the unconstrained and constrained cases under leftward and rightward lane change conditions. The results illustrate that the proposed MPC-based simultaneous trajectory planning and tracking approach achieves acceptable obstacle avoidance performance for an intelligent vehicle.**

***Index Terms*—Cyber-physical systems (CPSs), intelligent vehicle, model predictive control (MPC), obstacle avoidance, trajectory planning and tracking.**

Manuscript received September 26, 2017; revised January 3, 2018 and February 23, 2018; accepted February 27, 2018. Date of publication March 13, 2018; date of current version September 4, 2018. This work was supported by the National Nature Science Foundation of China (61520106008, 61790563). Paper no. TII-17-2225. *(Corresponding author: Hong Chen.)*

H. Guo, C. Shen, H. Chen, and R. Jia are with the State Key Laboratory of Automotive Simulation and Control and the Department of Control Science and Engineering, Jilin University, Changchun 130021, China (e-mail: guohongyan220@163.com; 987543592@qq.com; chenh@jlu.edu.cn; 707176842@qq.com).

H. Zhang is with the School of Transportation Science and Engineering, Beihang University, Beijing 100083, China (e-mail: huizhang285@gmail.com).

Color versions of one or more of the figures in this paper are available online at http://ieeexplore.ieee.org.

Digital Object Identifier 10.1109/TII.2018.2815531

I. Introduction

RAPID developments in hardware, software, and networking technologies have paved the way for cyber-physical systems (CPSs), which have received a great deal of attention from academia, industry, and the government due to their potential benefits to the society, the economy, and the environment [1]–[3]. CPSs are regarded as the next generation of engineered systems, in which computing, communication, and control technologies are tightly integrated to achieve stability, precision, reliability, robustness, and efficiency in dealing with physical systems in many application domains [4], [5]. Intelligent vehicles are a typical engineered system and contain the interactions among human driver, traffic environment, and automated control systems. They are a typical example of CPSs and have been receiving increasing attention due to their great potential for enhancing vehicle safety and performance, as well as traffic efficiency [6]. According to SAE J3016, intelligent vehicles can be divided into six levels of driving automation: no automation, driver assistance, partial automation, conditional automation, high automation, and full automation [7]. The obstacle avoidance problem for an intelligent vehicle, especially lateral obstacle avoidance, is tightly integrated with traffic environment, control technologies, and human drivers. It is a vital issue for the safety of intelligent transportation systems [8], and accordingly, it is a hot topic of discussion for researchers [9], [10].

From the perspective of control science, the obstacle avoidance problem for an intelligent vehicle once an obstacle has been detected can be described as a combined path/trajectory planning and tracking problem [11]. Several studies have already been conducted on path/trajectory planning and tracking problems, and such problems have been widely discussed. In [12], a vision algorithm was presented for detecting the reference path, and a nonlinear backstepping controller was designed for path tracking in an emergency obstacle avoidance situation. In [13], a neural-network-based intelligent planner was designed for moving obstacle avoidance. In [14], a homogeneity-based finite-time tracking control method was presented for the tracking control of an autonomous surface vehicle. The aforementioned methods can be used to effectively generate a reference path or

trajectory and to control an intelligent vehicle to follow that reference path/trajectory. However, realistic constraints on the actuator and the lateral displacement are not considered, and consequently, these methods can easily result in the saturation of the actuator or collision with the road boundary.

Model predictive control (MPC) is an appealing technique for intelligent vehicles due to its ability to handle constraints [15], [16]. Accordingly, it can be effectively employed to address the path/trajectory planning and tracking problem for intelligent vehicles. In [17], a moving horizon controller was proposed to address the path tracking problem for automated vehicles with road boundary constraints, and the desired path was obtained via cubic Lagrange interpolation based on the measured data. In [9], a two-stage nonlinear nonconvex MPC control approach for autonomous vehicle obstacle avoidance was developed by tracking the centerline of the roadway under highway cruise conditions. The aforementioned MPC methods can track an already-obtained path while simultaneously considering the constraints imposed on an intelligent vehicle. However, two controllers are required to solve the entire path/trajectory planning and tracking problem to achieve obstacle avoidance for the intelligent vehicle.

In this manuscript, a simultaneous trajectory planning and tracking controller for use under cruise conditions is presented that uses the MPC approach to address the obstacle avoidance problem for an intelligent vehicle, as an example of a typical CPS. The reference trajectory is parameterized as a cubic function in time and is determined by the lateral position and velocity of the intelligent vehicle and the velocity and yaw angle of the obstacle vehicle at the start point of the lane change maneuver. By using the lateral velocity of the intelligent vehicle at the end point of the lane change as an intermediate variable, the control input sequence for the vehicle is incorporated into the expression for the reference trajectory that is used in the MPC optimization problem, allowing both trajectory planning and tracking to be captured in a single MPC optimization problem. To verify the effectiveness of the proposed simultaneous trajectory planning and tracking approach, various validations conducted for both leftward and rightward lane change scenarios are presented.

The two main contributions of this paper are as follows.

1) An MPC-based simultaneous trajectory planning and tracking approach is proposed to achieve obstacle avoidance for an intelligent vehicle in the situation in which using the braking operation alone cannot prevent a collision and in which the other lane is available. The control sequence for the vehicle is incorporated into the reference trajectory expression that is used in the MPC optimization problem by using the lateral velocity of the intelligent vehicle at the end point of the lane change as an intermediate variable, thereby enabling simultaneous trajectory planning and tracking.
2) The reference trajectory is parameterized as a cubic function in time, and the desired lateral position is determined according to the position of the obstacle vehicle. Only the lateral position and velocity of the intelligent vehicle and the velocity and yaw angle of the obstacle vehicle at the start point of the lane change maneuver need to be known to generate the reference trajectory.

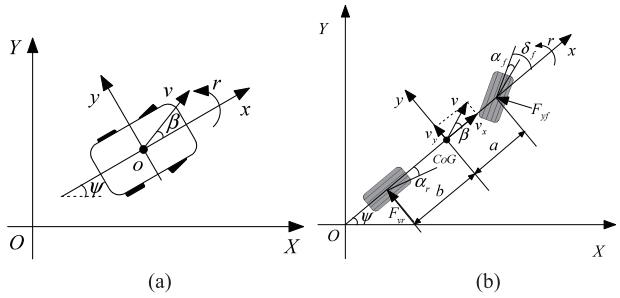

Fig. 1. Intelligent vehicle model used to define the obstacle avoidance problem. (a) Vehicle kinematic relations. (b) Vehicle dynamics model.

This paper is organized as follows. In Section II, the vehicle dynamics models of the obstacle vehicle and the intelligent vehicle are presented, and the obstacle avoidance problem is defined. In Section III, the proposed simultaneous trajectory planning and tracking approach is introduced. In Section IV, simulations conducted under different operating conditions are reported. Finally, in Section V, the conclusions are presented.

II. System Modeling and Problem Statement

In this study, both an intelligent vehicle model and an obstacle vehicle model have been developed for trajectory planning and tracking control. The intelligent vehicle model is used for the controller design, and the obstacle vehicle model is used to predict the future motion of the obstacles to be avoided.

A. Single-Track Model

Assuming that a vehicle is a rigid body with nondeformable wheels, the vehicle kinematics can be obtained in accordance with the geometric relationships illustrated in Fig. 1(a)

$$\dot{x}_o = v_x \cos(\psi + \beta) \tag{1a}$$

$$\dot{y}_o = v_x \sin(\psi + \beta) \tag{1b}$$

$$\dot{\psi} = r \tag{1c}$$

where x_o and y_o are the longitudinal and lateral positions of the center of gravity (CoG), r is the yaw rate, β is the sideslip angle, ψ is the yaw angle, and v_x is the longitudinal velocity. Considering that the variances in the yaw angle and the sideslip angle are small and that the road curvature is also small, it can be assumed that $\sin(\psi + \beta) \approx \psi + \beta$, $\cos(\psi + \beta) \approx 1$, and $\beta = \frac{v_y}{v_x}$, and the model can be simplified as

$$\dot{x}_o = v_x \tag{2a}$$

$$\dot{y}_o = v_x \psi + v_y \tag{2b}$$

$$\dot{\psi} = r. \tag{2c}$$

It is important to know the lateral dynamic states of the intelligent vehicle. As shown in Fig. 1(b), the vehicle body coordinate system is defined with the origin at the CoG. The positive direction of the x-axis points in the forward direction, the positive

direction of the y-axis points to the left, and the directions of the z-axis and other forces and torques are determined by the righthand rule. In accordance with the force and torque balance in the lateral direction, the lateral dynamics of the single-track vehicle can be derived as follows:

$$m(\dot{v}_y + r v_x) = F_{yf} + F_{yr} \tag{3a}$$

$$I_z \dot{r} = a F_{yf} - b F_{yr} \tag{3b}$$

where m is the mass of the vehicle; v_y is its lateral velocity; F_{yf} and F_{yr} are the lateral forces on the front and rear tires, respectively; I_z is the moment of inertia of the vehicle about the z-axis; and a and b are the distances from the CoG to the front and rear axles, respectively.

A linear tire model is employed to describe the lateral forces on the front and rear tires: $F_{yf} = C_f \alpha_f$, $F_{yr} = C_r \alpha_r$, where α_f and α_r are the sideslip angles and C_f and C_r are the cornering stiffness of the front and rear tires, respectively.

When the vehicle is operating under steady-state conditions, the sideslip angles α_f and α_r are so small that they can be assumed to satisfy $\tan\alpha_f \approx \alpha_f$ and $\tan\alpha_r \approx \alpha_r$. Therefore, the sideslip angles of the front and rear tires can be approximated as [18]: $\alpha_f = \frac{v_y + ar}{v_x} - \delta_f$, $\alpha_r = \frac{v_y - br}{v_x}$. Then, combining the result with (2), the lateral dynamics of the single-track vehicle can be described as follows:

$$\begin{aligned}
\dot{y}_o &= v_x \psi + v_y, \\
\dot{v}_y &= \frac{(C_f + C_r)}{m v_x} v_y + \left(\frac{(aC_f - bC_r)}{m v_x} - v_x \right) r - \frac{C_f}{m} \delta_f \\
\dot{r} &= \frac{(aC_f - bC_r)}{I_z v_x} v_y + \frac{(a^2 C_f + b^2 C_r)}{I_z} r - \frac{aC_f}{I_z v_x} \delta_f \\
\dot{\psi} &= r.
\end{aligned} \tag{4}$$

Normally, the steering ratio, which is defined as the ratio of the steering wheel rotation angle to the steering angle at the wheels, ranges from 15 or 20 to 1 on passenger cars. Because of the compliance and steering torque gradients with increasing steering angles, the actual steering ratio may be as high as twice the design ratio [19]. Considering that modeling error can be effectively suppressed by feedback control, the description of the relationship between the front wheel steering angle δ_f and the steering wheel angle δ_{sw} in [20] is adopted, where the steering wheel angle can be expressed as $\delta_{\text{sw}} = I_s \delta_f$. By selecting the lateral position as the output and the steering wheel angle as the input and expressing the states in the form $x = [y_o \; v_y \; r \; \psi]$, the state-space description of the single-track vehicle shown in (4) can be formulated as follows:

$$\dot{x} = Ax + B\delta_{\text{sw}} \tag{5a}$$

$$y = Cx \tag{5b}$$

where

$$\boldsymbol{A} = \begin{bmatrix} 0 & 1 & 0 & v_x \\ 0 & \frac{C_f + C_r}{m v_x} & \frac{aC_f - bC_r}{m v_x} - v_x & 0 \\ 0 & \frac{aC_f - bC_r}{I_z v_x} & \frac{a^2 C_f + b^2 C_r}{I_z v_x} & 0 \\ 0 & 0 & 1 & 0 \end{bmatrix}, \boldsymbol{B} = \begin{bmatrix} 0 \\ -\frac{C_f}{I_{\text{sw}} m} \\ -\frac{aC_f}{I_z I_{\text{sw}}} \\ 0 \end{bmatrix}, \boldsymbol{C} = \begin{bmatrix} 1 \\ 0 \\ 0 \\ 0 \end{bmatrix}^{\text{T}}.$$

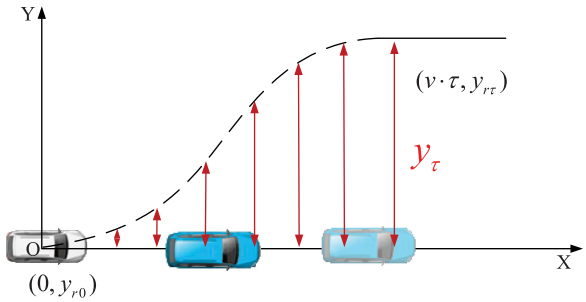

Fig. 2. Schematic diagram of obstacle avoidance by an intelligent vehicle.

By discretizing (5) with a sampling interval T_s using the zero-order hold approach, the following discrete-time model can be obtained:

$$\begin{aligned}
x(k+1) &= A_d x(k) + B_d \delta_{\text{sw}}(k) \\
y(k) &= C_d x(k)
\end{aligned} \tag{6}$$

where $A_d = e^{AT_s}$, $B_d = \int_0^{T_s} e^{A\tau} d\tau \cdot B$, and $C_d = C$ are the discrete-time matrices.

B. Obstacle Vehicle Model

To guarantee safe trajectory planning, both the current and future motion of the obstacle vehicle should be considered. However, the future motion of the obstacle vehicle is generally unknown, so it is important to be able to effectively predict its future states. The yaw angle, velocity, and angular velocity of the obstacle vehicle can be measured by the camera, which was produced by the Mobileye company. The identification time of the camera is 40 s [21], which is less than the control period of the intelligent vehicle, which is 50 ms [22]. To this end, under the assumption that the yaw angle, velocity, and angular velocity of the obstacle vehicle can be measured, this vehicle can be described in the following discrete form:

$$X_{\text{obs}}(k+1) = X_{\text{obs}}(k) + T_s \cos\theta_{\text{obs}}(k) v_{\text{obs}}(k) \tag{7a}$$

$$Y_{\text{obs}}(k+1) = Y_{\text{obs}}(k) + T_s \sin\theta_{\text{obs}}(k) v_{\text{obs}}(k) \tag{7b}$$

$$\theta_{\text{obs}}(k+1) = \theta_{\text{obs}}(k) + T_s \omega_{\text{obs}}(k) \tag{7c}$$

where $X_{\text{obs}}(k)$ and $Y_{\text{obs}}(k)$ are the longitudinal and lateral the position coordinate at time k of the obstacle vehicle, $v_{\text{obs}}(k)$ is its current velocity at time k, $\theta_{\text{obs}}(k)$ is its current yaw angle, ω_{obs} is its current yaw rate, and T_s is the sampling interval.

C. Obstacle Avoidance Problem Statement

As an example of an obstacle avoidance scenario whereby there is an obstacle vehicle in front of the intelligent vehicle and whereby the left road is available for lane changing, the intelligent vehicle must change lanes when a collision cannot be avoided through braking alone. As shown in Fig. 2, the simultaneous trajectory planning and tracking controller takes over the steering operation when the braking operation by the driver is not sufficient in an emergency, and a leftward lane change of an

intelligent vehicle for obstacle avoidance is adopted. The safe distance is used to determine when lane changing is necessary and is related to the relative velocity between the intelligent vehicle and the obstacle vehicle. The following safe distance is employed [23]:

$$D = \frac{v_x^2}{2a_{\max}} - \frac{v_{\text{obs}}^2}{2a_{\max,\text{obs}}} + v_x t_1 + d_0 \tag{8}$$

where v_x is the longitudinal velocity of the intelligent vehicle, v_{obs} is the velocity of the obstacle vehicle, $a_{\max}$ is the maximum deceleration of the intelligent vehicle, $a_{\max,\text{obs}}$ is the maximum deceleration of the obstacle vehicle, t_1 is the detection and response time, and d_0 is the minimum distance between two cars. Considering that the obstacle is likely to stop in an emergency, v_{obs} is set to be 0. The safe distance is used as an analysis condition for changing lanes, and other definitions of the safe distance, such as the safe distance in [24] and [25], could similarly be used for this purpose.

To complete the lane change, the intelligent vehicle must track the desired trajectory as shown in Fig. 2 and the obstacle avoidance problem can be described as a trajectory tracking issue. The start point of the lane change maneuver is denoted by $(0, y_{ro})$, and the end point is denoted by $(v \cdot \tau, y_{r\tau})$. The lateral displacement of the intelligent vehicle between the start and end points is determined based on the motion of the obstacle vehicle and is denoted by $y_{r\tau}$. To avoid a collision with the obstacle vehicle, a safety margin is added to the lateral displacement of the obstacle vehicle to obtain the desired lateral displacement of the intelligent vehicle: $y_{r\tau} = Y_{\text{obs},\tau} + y_\tau$, where $y_{r\tau}$ is the lateral displacement of the intelligent vehicle at time τ; y_τ is the safe lateral distance, which should satisfy $y_\tau \le v_{\text{obs}} \sin\theta_{\text{obs}}\tau + \frac{1}{2}a_{y,\text{obs}}\tau^2$; and $Y_{\text{obs},\tau}$ is the lateral displacement of the obstacle vehicle at time τ. The lateral displacement of the obstacle vehicle at time τ can be predicted using (7b), and it describes the behavior of the human driver in the obstacle vehicle in the lateral direction.

III. MPC-Based Simultaneous Trajectory Planning and Tracking Controller Design

Many control approaches have been applied to address the trajectory planning and tracking problem [26]–[28]. Because the traffic conditions and the motions of the obstacle vehicles ahead are constantly varying, an intelligent vehicle must be able to react suitably at each sampling instant. An intelligent vehicle usually reacts by planning a feasible trajectory, and then, tracking that trajectory, which typically requires two controllers. In this manuscript, an MPC approach is introduced that can perform trajectory planning and tracking simultaneously. A diagram of the proposed controller design is presented in Fig. 3. The strategy includes four tasks: computation of the desired lateral displacement, prediction of the intelligent vehicle states and output, generation of the desired trajectory, and optimization.

A. State and Output Prediction for the Intelligent Vehicle

Considering that the longitudinal velocity may change during the lane change maneuver, it is assumed that the longitudinal

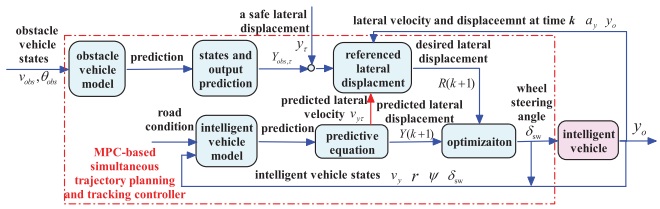

Fig. 3. Design of the simultaneous trajectory planning and tracking controller.

velocity v_x remains invariant during the predictive horizon. Thus, the system matrices A and B in (5a) can be assumed as time invariant in the predictive horizon. In the next sample time, the variation in the longitudinal velocity v_x is considered, and the description of the system matrices A and B in (5a) is updated. Moreover, it is assumed that the velocity, yaw angle, sideslip angle, and tire-road friction coefficient of the vehicle can be straightforwardly obtained by estimation schemes in [29], where an early detection algorithm of the friction coefficient using only the signal when the vehicle is decelerating mildly is introduced.

Suppose that the predictive horizon is p, the control horizon is m, and $m \le p$. For sampling instants that lie beyond the control horizon m, it is assumed that the control input remains invariant, that is, $u(k+m) = u(k+m+1) = \cdots = u(k+p-1)$. According to the system dynamics described in (6), let the control input sequence $U(k)$ and the predicted output sequence $Y(k+1|k)$ at sampling instant k be defined as follows:

$$U(k) \triangleq \begin{bmatrix} \delta_{sw}(k) \\ \delta_{sw}(k+1) \\ \vdots \\ \delta_{sw}(k+m-1) \end{bmatrix}, Y(k+1|k) \triangleq \begin{bmatrix} y(k+1|k) \\ y(k+2|k) \\ \vdots \\ y(k+p|k) \end{bmatrix}.$$

Accordingly, the p-step output prediction for the intelligent vehicle can be expressed as follows:

$$Y(k+1|k) = S_x x(k) + S_u U(k) \tag{9}$$

where $S_x = \begin{bmatrix} C_d A_d & C_d A_d^2 & \cdots & C_d A_d^p \end{bmatrix}^T$ and

$$S_u = \begin{bmatrix} C_d B_d & 0 & \cdots & 0 \\ C_d A_d B_d & C_d B_d & \cdots & 0 \\ \vdots & \vdots & \ddots & \vdots \\ C_d A^{p-1} B_d & C_d A^{p-2} B_d & \cdots & \sum_{i=1}^{p-m+1} C_d A_d^{i-1} B_d \end{bmatrix}.$$

B. Trajectory Generation

The obstacle avoidance problem can be divided into longitudinal velocity control and lateral position control. When the longitudinal velocity is determined, the longitudinal position can be computed. Considering that we are discussing obstacle avoidance based on steering operations, the longitudinal position is computed from the longitudinal velocity directly. Thus, the intelligent vehicle can be described by (5a). In addition, the intelligent vehicle is regarded as a typical system with nonholonomic constraints, whose yaw angle and trajectory must be

continuous at all times. Thus, a parametric cubic polynomial in terms of the time variable is adopted to represent the desired lateral displacement

$$y_r(t) = b_3t^3 + b_2t^2 + b_1t + b_0 \tag{10}$$

where y_r denotes the desired lateral displacement and b_3, b_2, b_1, and b_0 are coefficients to be determined.

For a time interval $[0, \tau]$, the boundary conditions on the vehicle's lateral displacements at the initial and final times can be described as follows:

$$y_r(0) = y_0, y_r(\tau) = y_{r\tau}, \dot{y}_r(0) = v_{y0}, \dot{y}_r(\tau) = v_{y\tau} \tag{11}$$

where y_0 and y_τ are the initial and final lateral displacements, respectively, of the intelligent vehicle in the time interval $[0, \tau]$, and v_{y0} and $v_{y\tau}$ are the vehicle's initial and final lateral velocities in this time interval.

The derivative of the lateral displacement $y_r(t)$ with respect to time t can be obtained as follows:

$$\dot{y}_r(t) = 3b_3t^2 + 2b_2t + b_1. \tag{12}$$

Then, by substituting the boundary conditions given in (11) into (10) and (12), the coefficients b_3, b_2, b_1, and b_0 in (10) can be determined as follows:

$$b_0 = y_0,\ b_2 = -\frac{3}{\tau^2}y_0 + \frac{3}{\tau^2}y_{r\tau} - \frac{2}{\tau}v_{y0} - \frac{1}{\tau}v_{y\tau} \tag{13a}$$

$$b_1 = v_{y0},\ b_3 = \frac{2}{\tau^3}y_0 - \frac{2}{\tau^3}y_{r\tau} + \frac{1}{\tau^2}v_{y0} + \frac{1}{\tau^2}v_{y\tau}. \tag{13b}$$

Thus, the desired lateral trajectory of the intelligent vehicle can be determined under the condition that the lateral displacement and velocity at the initial and final times of the time interval $[0, \tau]$ are already known. However, it should be noted that the lateral velocity of the intelligent vehicle at the end point cannot, in fact, be obtained, and thus, the desired lateral trajectory is still undetermined at this point.

Now, by discretizing the trajectory of the intelligent vehicle given in (10) with a sampling interval of T_s, and substituting (13) into the discrete form of (10), the trajectory can be expressed as $y_r(k+i|k) = [(\frac{2y_0 - 2y_{r\tau} + \tau v_{y0}}{\tau^3})(i \cdot T_s)^3 + (\frac{3y_0 + 3y_{r\tau} - 2\tau v_{y0}}{\tau^2})(i \cdot T_s)^2 + v_{y0}(i \cdot T_s) + y_0] + [\frac{1}{\tau^2}(i \cdot T_s)^3 - \frac{1}{\tau}(i \cdot T_s)^2]\, v_{y\tau}$. By considering the lateral displacement $y(k+i|k)$ that is computed for the time interval $[kT_s, (k+i)T_s]$, the following formulations can be straightforwardly determined: $y_0 = y(k)$ and $v_{y0} = v_y(k)$. To simplify the aforementioned expression, the following substitutions are adopted $m_0 = y_0$, $m_1 = v_{y0}$, $m_{21} = -\frac{3y_0}{\tau^2} + \frac{3y_{r\tau}}{\tau^2} - \frac{2v_{y0}}{\tau}$, $m_{22} = -\frac{1}{\tau}$, $m_{31} = \frac{2y_0}{\tau^3} - \frac{2y_{r\tau}}{\tau^3} + \frac{v_{y0}}{\tau^2}$, and $m_{32} = \frac{1}{\tau^2}$. Thus, the lateral displacement described previously can be rewritten as

$$y_r(k+i|k) = [m_{31}(i \cdot T_s)^3 + m_{21}(i \cdot T_s)^2 + m_1(i \cdot T_s) + m_0] + [m_{32}(i \cdot T_s)^3 + m_{22}(i \cdot T_s)^2]v_{y\tau} \tag{14}$$

where $v_{y\tau}$ is the lateral velocity at the final time instant of the predictive horizon. Let $\tau = p \cdot T_s$; then, this lateral velocity can be computed as follows:

$$v_{y\tau} = C_{v_y} x_\tau \tag{15}$$

where $C_{v_y} = [0\,1\,0\,0]$. In addition, $x_\tau = x(k+p|k)$ is the state of the intelligent vehicle at the final time instant of the predictive horizon, and it can be written as follows:

$$x_\tau = G_x x(k) + G_u U(k) \tag{16}$$

where $G_u = \left[\, A_d^{p-1}B_d\ A_d^{p-2}B_d\ \cdots\ A_d^{p-m}B_d \,\right]$ and $G_x = A_d^p$. The main control requirement is that the intelligent vehicle should track the reference trajectory as closely as possible; thus by substituting (15) and (16) into (14), the desired reference trajectory can be defined as follows:

$$R_y(k+1) = R + R_x x(k) + R_u U(k) \tag{17}$$

where $R = [r_1\ r_2\ \cdots\ r_p\,]^T$, $R_x = [\,r_{x1}\ r_{x2}\ \cdots r_{xp}]^T$, $R_u = [\,r_{u1}\ r_{u2}\ \cdots\ r_{up}\,]$, $r_i = m_{31}(i \cdot T_s)^3 + m_{21}(i \cdot T_s)^2 + m_1 + m_0$, $r_{xi} = [m_{32}(i \cdot T_s)^3 + m_{22}(i \cdot T_s)^2]C_{v_y} G_x$, and $r_{ui} = [m_{32}(i \cdot T_s)^3 + m_{22}(i \cdot T_s)^2]C_{v_y} G_u$, $i = 1, 2, \cdots, p$.

It can be seen from (14)–(17) that the reference trajectory can be obtained in a novel manner if the lateral position and velocity of the intelligent vehicle and the velocity and yaw angle of the obstacle vehicle at the start point of the lane change maneuver can be obtained. The velocity and acceleration information of the final point for the intelligent vehicle is unnecessary. Moreover, the control input sequence is contained in the desired trajectory, as can be seen from (17), which makes the simultaneous trajectory planning and tracking possible. The aforementioned advantages are the main novelty of this obstacle avoidance scheme.

C. Unconstrained Optimization

The unconstrained MPC can obtain an optimal value, and the computation time is much lower than in the constrained case. This motivates us to discuss the unconstrained case first. To make the intelligent vehicle follow the desired trajectory, it is necessary to minimize the difference between the predicted lateral displacement of the intelligent vehicle as expressed in (9) and the desired trajectory as expressed in (17), which can be described as minimizing the trajectory tracking error: $J_1 = \|Y(k+1|k) - R_y(k+1)\|$.

In addition, to restrict large control action in a sample time, the steering action of the steering wheel motor should be limited. The corresponding requirement is formulated as the minimization of $J_2 = \|U(k)\|$.

Because it is impossible to minimize J_1 and J_2 simultaneously, weighting factors are introduced. Thus, the multiobjective cost function over a receding horizon is defined

$$\min_{U(k)}\ J(y(k), U(k), m, p) \tag{18a}$$

$$J = \|\Gamma_y(Y(k+1 \mid k) - R(k+1)\| + \|\Gamma_u U(k)\| \tag{18b}$$

where $J(y(k), U(k), m, p)$ is the cost function and $\Gamma_y = \mathrm{diag}(\Gamma_{y,1}, \Gamma_{y,2}, \ldots, \Gamma_{y,p})$ and $\Gamma_u = \mathrm{diag}(\Gamma_{u,1}, \Gamma_{u,2}, \ldots, \Gamma_{u,m})$ are the weighting matrices.

Upon substituting (9) and (17) into (18b), let the partial derivative of the cost function J with respect to the control input sequence $U(k)$ be equal to zero, that is, $\frac{\partial J}{\partial U(k)} = 0$. Then, the corresponding extreme solution for the control input sequence

is obtained as follows:

$$U^*(k) = [(S_u - R_u)^T \Gamma_y^T \Gamma_y (S_u - R_u) + \Gamma_u^T \Gamma_u]^{-1} (S_u - R_u)^T \Gamma_y^T \Gamma_y E_p(k+1\,|k) \tag{19}$$

where $E_p(k+1\,|k) = R_y(k+1) - (S_x - R_x)x(k)$.

Considering that the second-order partial derivative of the cost function J with respect to the control input sequence $U(k)$ is $\frac{\partial^2 J}{\partial U^2(k)} = 2[(S_u - R_u)^T \Gamma_y^T \Gamma_y (S_u - R_u) + \Gamma_u^T \Gamma_u] > 0$, it can be concluded that the solution given in (19) results in the minimal value of (18). Thus, the optimal solution to the optimization problem defined in (18) can be found.

Once the aforementioned optimization problem has been solved, the first element of the optimal control sequence $U(k)$ is applied to the intelligent vehicle system. Hence, at time instant k, the resulting state feedback control law is

$$\delta_{\text{sw}}^{\star} = [\,1,\ 0,\ \cdots\ 0\,]U(k) \tag{20}$$

where $\delta_{\text{sw}}^{\star}(k)$ is the optimal vector of steering wheel angles and serves as the control signal to the intelligent vehicle system. In the next time instant, the predictive horizon is moved forward one interval, and the optimization problem is solved again using the newly recorded process measurements.

Remark 3.1: It design, and derivation presented previously are based on a leftward lane change scenario. The design process for the rightward lane change scenario is similar to that for the leftward lane change scenario. The only difference lies in the generation of the desired trajectory. When the vehicle must perform a rightward lane change, the formula for the lateral displacement at time τ must be rewritten as $y_{r\tau} = Y_{\text{obs},\tau} - y_\tau$. The subsequent derivation of the MPC-based simultaneous trajectory planning and tracking controller is identical to the design process presented previously.

D. Constrained Case

To avoid collision with the road boundary or other vehicles, the lateral displacement of the intelligent vehicle should be constrained such that it remains within the lane lines. Therefore, the following constraints on the lateral displacement should be considered:

$$y_{\min}(k) \le y(k) \le y_{\max}(k)\ \forall k \ge 0 \tag{21}$$

where $y_{\min}$ and $y_{\max}$ are the minimum and maximum allowed lateral displacements, respectively, of the intelligent vehicle.

In addition, the mechanical characteristics of the steering system place bounds on the feasible steering variation. To ensure the practicality of the control variable, the following constraints on the control input sequence should be considered:

$$\delta_{\text{sw},\min}(k) \le \delta_{\text{sw}}(k) \le \delta_{\text{sw},\max}(k)\ \forall k \ge 0 \tag{22}$$

where $\delta_{\text{sw},\min}$ and $\delta_{\text{sw},\max}$ are the minimum and maximum allowed steering wheel angles, respectively.

According to the objective function defined in (18b) and the constraints formulated in (21) and (22), the MPC optimization problem for simultaneous trajectory planning and tracking in the constrained case is as follows:

$$\min_{U(k)} J(y(k), U(k), m, p)$$
$$\text{s.t. } (6), (21), (22), \text{ and } x(k|k) = x(k) \tag{23}$$

By synthesizing the cost function in (18b), output constraint in (21) and input constraint in (22), the constrained optimization problem for MPC-based simultaneous trajectory planning and tracking can finally be transformed into the quadratic programming problem. Then, the first element of the optimal control sequence can be applied to the intelligent vehicle, and thus, trajectory planning and tracking can be achieved simultaneously.

IV. Results and Discussions

To verify the effectiveness of the proposed MPC-based obstacle avoidance method, simulations were conducted under various operating conditions using the high-precision model of the Hongqi HQ430 vehicle implemented in the high-fidelity software package veDYNA. The parameters of the Hongqi HQ430 vehicle used here can be referred to [17]. The relationship between the predictive horizon and the control horizon should satisfy $m \le p$. Actually, the larger the chosen predictive horizon, the greater the amount of information obtained regarding future intelligent vehicle dynamics. As a result, better obstacle avoidance performance can be obtained. On the other hand, a larger predictive horizon implies a longer computation time for MPC. In addition, the larger the control horizon selected, the smoother the control action obtained. On the other hand, a relatively long computation time is required to solve the optimization problem. Therefore, the choice of the predictive horizon represents a tradeoff between obstacle avoidance performance and the computation time of the MPC controller. Based on the aforementioned consideration, the predictive and control horizons were selected to be $p = 10$ and $m = 8$, respectively. The minimum and maximum lateral displacements were chosen to be $y_{\min} = -1$ and $y_{\max} = 4.1$, respectively, in accordance with the lane line geometry. The minimum and maximum steering wheel angles were selected to be $\delta_{\text{sw},\min} = -0.52$ and $\delta_{\text{sw},\max} = 0.52$, respectively, based on the steering characteristics of the intelligent vehicle traveling at high velocity. In addition, it is known that a larger Γ_y results in smaller tracking errors, implying larger control actions $U(k)$. Similarly, a larger Γ_u results in smaller control actions. Thus, Γ_y and Γ_u have conflicting effects on the minimization of the objective function. Consequently, when defining the weighting matrices, a compromise must be established between following the desired trajectory and limiting the actuator action. In this study, the weighting matrices were determined to be $\Gamma_y = \text{diag}(0.41,\ 0.41,\ \cdots,\ 0.41)$ and $\Gamma_u = \text{diag}(0.6,\ 0.6,\ \cdots,\ 0.6)$ based on regulation rules in [15].

A. Leftward Lane Change Simulation

To verify the obstacle avoidance performance of the proposed MPC-based trajectory planning and tracking controller, a simulation was conducted under leftward lane change conditions on an asphalt road with a coefficient of friction of $\mu = 0.9$. In this scenario, the intelligent vehicle accelerates from stationary

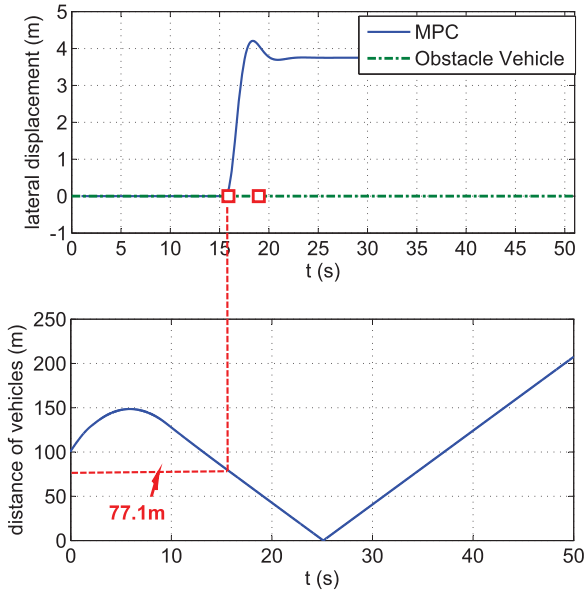

Fig. 4. Simulation results of the lateral displacement and vehicle separation distance for the leftward lane change scenario.

to a speed of 90 km/h. Then, it cruises at a constant velocity of 90 km/h while remaining in its lane. There is an obstacle vehicle 100-m ahead of the intelligent vehicle and traveling straight forward at a velocity of 60 km/h. When the distance between the two vehicles has decreased to less than the safe distance computed using (8), the intelligent vehicle should change lanes using the proposed controller. The simulation results for this scenario are shown in Figs. 4 and 5(a)–(c).

It is seen from Fig. 4 that the distance between the intelligent vehicle and the obstacle vehicle initially increases as the intelligent vehicle begins to accelerate. Then, the distance between the two vehicles begins to decrease as the velocity of the intelligent vehicle increases. When the distance between the two vehicles is less than 77.1 m, as computed using (8), the intelligent vehicle chooses to change lane. In this case, the lateral displacement shown in Fig. 4 is generated. Moreover, the distance between the two vehicles continues to decrease because the velocity of the intelligent vehicle is higher than that of the obstacle vehicle. Once the lane change is complete, the distance between the two vehicles first becomes small, and then, gradually becomes larger as the intelligent vehicle overtakes the obstacle vehicle. The relative position of the two vehicles is also shown in Fig. 4, expressed using a rectangle. The results indicate that the intelligent vehicle can successfully avoid colliding with the obstacle vehicle. They also verify that the MPC approach is effective for simultaneous trajectory planning and tracking to allow an intelligent vehicle to avoid obstacles.

The optimized steering wheel angle obtained by solving the optimization problem defined in (19) is shown in Fig. 5(a), from which it can be seen that the maximum steering wheel angle of the intelligent vehicle during the lane change is approximately 0.6 radians. The lateral acceleration produced during the leftward lane change is less than 0.4 g, as shown in Fig. 5(b). This finding indicates that the intelligent vehicle remains

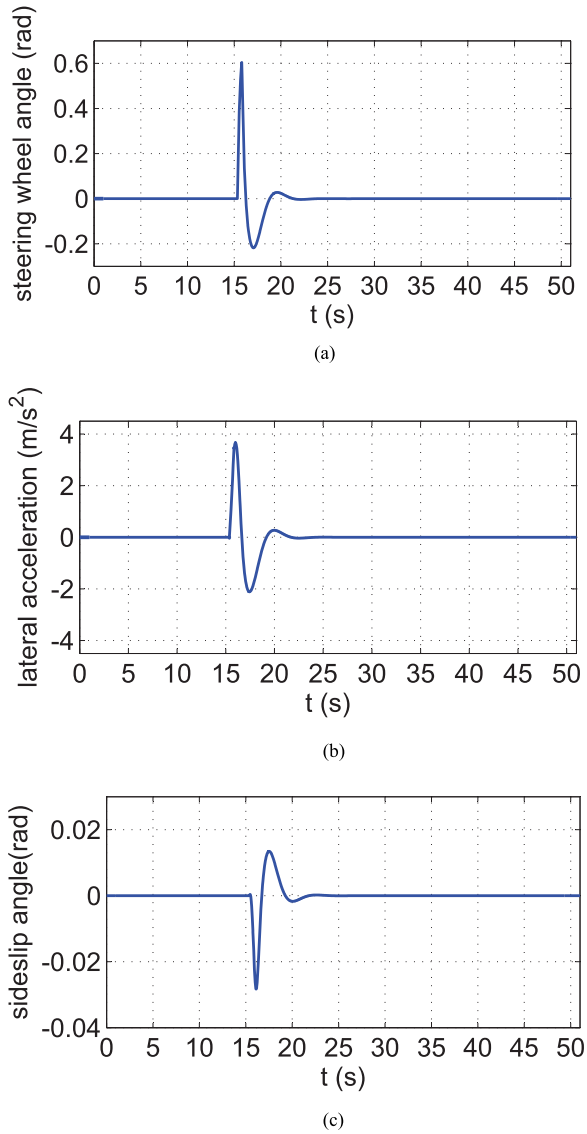

Fig. 5. Simulation results for the leftward lane change scenario. (a) Optimized steering wheel angle. (b) Lateral acceleration. (c) Sideslip angle.

laterally stable during the process of changing lanes. In addition, the sideslip angle remains less than 0.04 radians, as shown in Fig. 5(c). From these results, it can be further confirmed that the intelligent vehicle remains stable during the lane change. All of these simulation results verify that the proposed MPC-based simultaneous trajectory planning and following approach can effectively avoid collision with the obstacle vehicle while maintaining the lateral stability of the intelligent vehicle during the lane changing process.

B. Scenarios With Varying Velocities

To further validate the obstacle avoidance performance of the MPC-based simultaneous trajectory planning and tracking approach, simulations were conducted at various velocities. In these scenarios, the intelligent vehicle accelerates to a speed of 100, 110, or 120 km/h. The other operating conditions

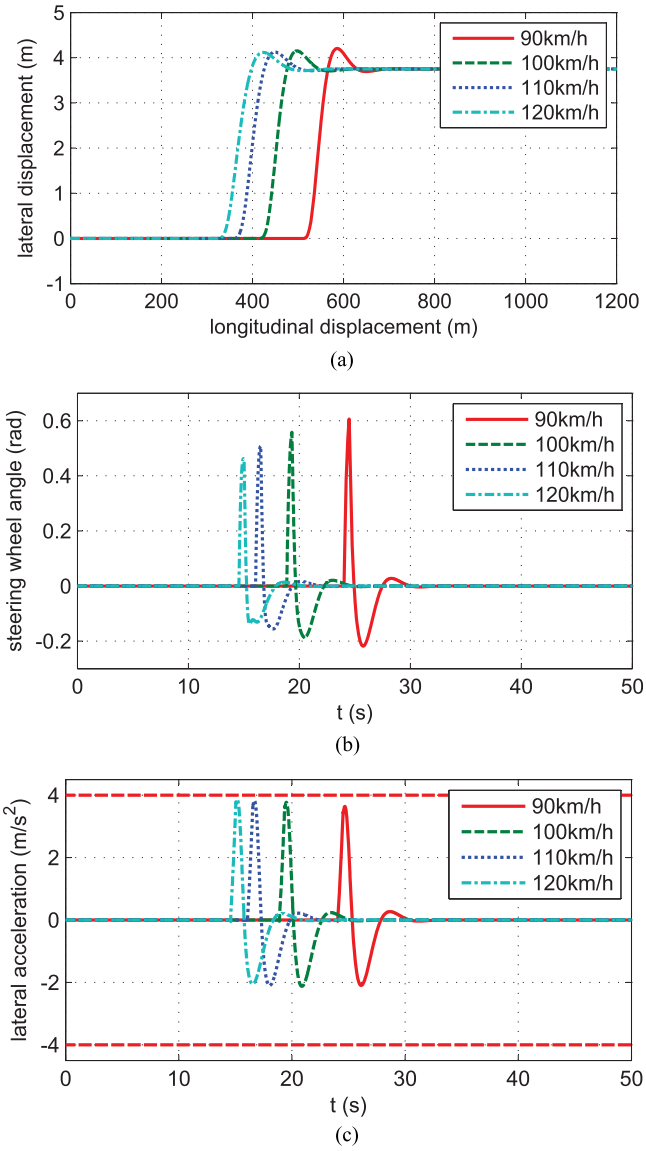

Fig. 6. Simulation results for various vehicle velocities. (a) Lateral displacement. (b) Optimized steering wheel angle. (c) Lateral acceleration.

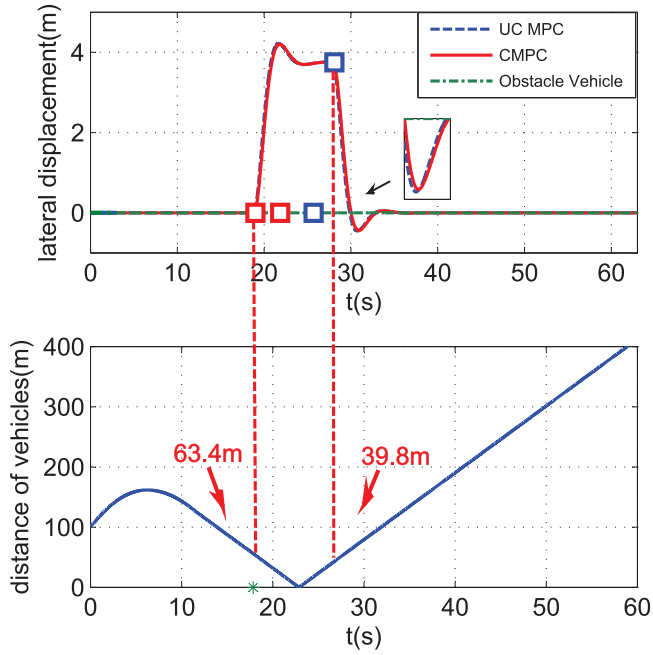

Fig. 7. Lateral displacement and vehicle separation distance during a double lane change maneuver; "UC MPC" denotes unconstrained MPC and "C MPC" denotes the constrained MPC.

remain the same as in the leftward lane change scenario described previously. The lateral displacement, steering wheel angle, lateral acceleration, and sideslip angle are shown in Fig. 6(a)–(c), respectively.

It is seen from Fig. 6(a) that the lane change maneuver is performed sooner as the velocity of the intelligent vehicle increases. The reason is that the safe distance computed using (8) becomes larger as the velocity of the intelligent vehicle increases. Additionally, as seen from the steering wheel angle shown in Fig. 6(b), when the velocity of the intelligent vehicle is higher, the maximum optimized steering wheel angle that is necessary to complete the lane change is smaller. This is because the steering ratio decreases with increasing velocity. It can be concluded from Fig. 6(a) and (b) that the proposed approach can successfully avoid collision with the obstacle vehicle for intelligent vehicles traveling at different velocities. Moreover, it can be seen from Fig. 6(c) that the lateral acceleration still remains below 0.4 g at all considered velocities. It confirm that the vehicle remains stable during obstacle avoidance at different velocities. From the simulation results shown in Fig. 6(a)–(c), it can be concluded that the proposed simultaneous trajectory planning and tracking approach can safely prevent collisions with obstacle vehicles for intelligent vehicles traveling at different velocities. We also verified the obstacle avoidance performance achieved by varying the tire–road friction coefficient. The results illustrate that the proposed simultaneous trajectory planning and tracking method can achieve acceptable obstacle avoidance performance for tire-road friction coefficients within a suitable range. Due to space limitation, the results were not listed here.

C. Validation and Comparison for the Constrained Case

To validate the effectiveness of the proposed MPC-based obstacle avoidance approach in the constrained case, the results of the simultaneous trajectory planning and tracking method considering the constraints on the steering wheel angle and lateral displacement are compared with the results obtained in the unconstrained case. In the scenario considered here, the intelligent vehicle accelerates from stationary to a velocity of 80 km/h on a road with a tire–road friction coefficient of $\mu = 0.9$. There is an obstacle vehicle traveling ahead of the intelligent vehicle at a velocity of 60 km/h. When the distance between the two vehicles becomes less than the safe distance, which is computed to be 80 m, the intelligent vehicle moves into the left lane. However, there is another obstacle vehicle traveling at a velocity of 60 km/h in the lane into which the intelligent vehicle has moved;

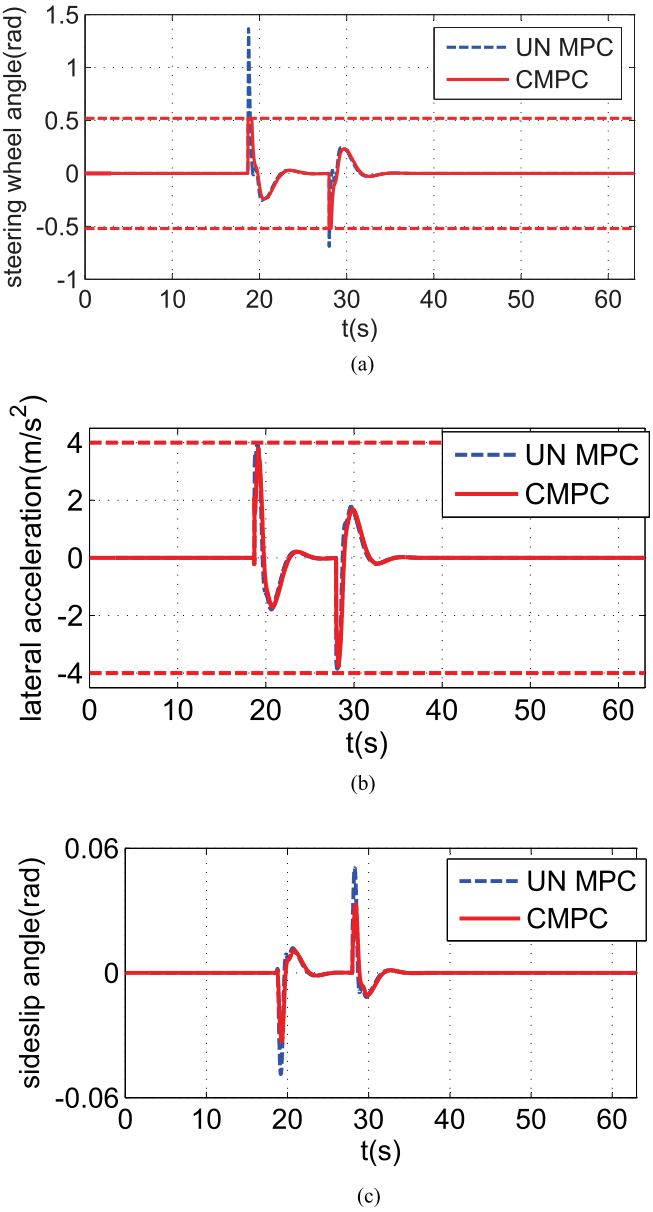

Fig. 8. Simulation results for the comparison of the constrained situation and the unconstrained situation; "UC MPC" denotes unconstrained MPC and "C MPC" denotes the constrained MPC. (a) Optimized steering wheel angle. (b) Lateral acceleration. (c) Sideslip angle.

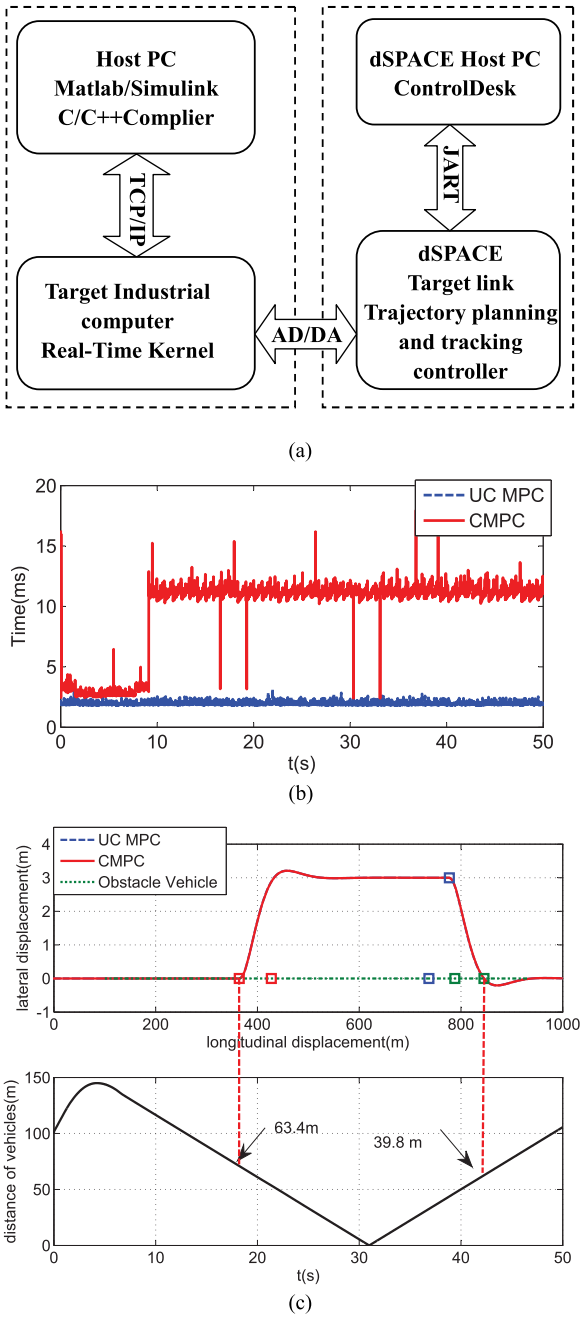

Fig. 9. Real-time performance validation for the comparison of the constrained and unconstrained situation; "UCMPC" denotes unconstrained MPC and "CMPC" denotes the constrained MPC. (a) Implementation scheme based on xPC-Target and dSPACE. (b) Computational time. (c) Trajectory.

therefore, the intelligent vehicle again moves into the right lane when the distance between these two vehicles becomes less than the computed safe distance. The simulation results are shown in Figs. 7 and 8(a)–(c).

As shown in Fig. 7, the intelligent vehicle achieves obstacle avoidance by moving into the left lane, and then, moving into the right lane to avoid colliding with the obstacle vehicles. The results verify that the proposed simultaneous trajectory planning and tracking approach is effective in both leftward and rightward lane change scenarios. They also further confirm that the proposed MPC-based approach can be successfully used for obstacle avoidance for intelligent vehicles.

Furthermore, the optimized steering wheel angle obtained under the corresponding input constraints is smaller than those obtained in the unconstrained case, as shown in Fig. 8(a). In addition, it can be concluded from the lateral acceleration results shown in Fig. 8(b) and the sideslip angle results shown in Fig. 8(c) that the intelligent vehicle remains stable during the lane changing process regardless of whether the steering wheel angle and lateral displacement constraints are considered. The findings presented previously demonstrate that the proposed simultaneous trajectory planning and tracking approach is feasible for obstacle avoidance regardless of whether constraints

are considered. The constrained MPC-based simultaneous trajectory planning and tracking approach is more effective for obtaining smaller lateral displacements, at the cost of a higher complexity of the optimization problem than in the unconstrained case. When choosing the more suitable control scheme for an intelligent vehicle, the tradeoff between the required lateral displacement and the complexity of the optimization problem should be considered.

D. Computational Performance Validation

To verify the real-time performance, the proposed approach is implemented and validated based on the xPC-Target and dSPACE. The Hongqi vehicle HQ430 runs in the target PC, and the simultaneous trajectory planning and tracking controller is implemented in the dSPACE. The PCL 818L and PCL 726 are used to communicate between the target PC and dSPACE by A/D and D/A data transportation. A detailed description of the experimental platform can be found in Fig. 9(a). The running condition is the same as the validation with the constrained case.

The computation time of the proposed MPC-based simultaneous trajectory planning and tracking controller is shown in Fig. 9(b). Both the unconstrained and constrained case of the proposed controller are solved in less than 50 ms. This verifies that the real-time performance can be achieved under the control requirements of the intelligent vehicle [22]. Moreover, it can be concluded that the computation time of the unconstrained MPC-based trajectory planning and tracking controller is less than that of the constrained MPC approach. This is because the unconstrained MPC can obtain an optimal value described in (19), and the constrained case needs to solve the quadratic programming optimization problem shown in (23). In addition, according to the results shown in Fig. 9(c), the obstacle avoidance performance is further validated by the real-time experiment and will hopefully be validated by real vehicle tests.

V. Conclusion

In this paper, an MPC-based simultaneous trajectory planning and tracking approach for obstacle avoidance by an intelligent vehicle is proposed. The reference trajectory is determined by both the lateral position and velocity of the intelligent vehicle and the velocity and yaw angle of the obstacle vehicle at the start point of the lane change maneuver, and it is parameterized as a cubic function in time. By using the predicted lateral velocity of the intelligent vehicle at the end point of the lane change as an intermediate variable, the control input sequence is incorporated into the expression for the reference trajectory that is used in the MPC optimization problem, thereby allowing both trajectory planning and tracking to be captured in a single MPC optimization problem. The proposed simultaneous trajectory planning and tracking method has been confirmed to be an effective means of achieving obstacle avoidance for intelligent vehicles in both the unconstrained and constrained cases.

In future research, a high-precision nonlinear vehicle model should be used to predict the motion of the obstacle vehicle. Further extensions of the simultaneous path planning and tracking MPC algorithm to the nonlinear case should be considered. The safe distance between the intelligent vehicle and the obstacle vehicle should be discussed in details. Moreover, a simultaneous trajectory planning and tracking approach that considers the driver steering behavior will be discussed.

References

[1] A. O. de Sá, L. F. da Costa Carmo, and R. C. S. Machado, "Covert attacks in cyber-physical control systems," *IEEE Trans. Ind. Informat.*, vol. 13, no. 4, pp. 1641–1651, Aug. 2017.

[2] V. Jirkovsyý, M. Obitko, and V. Mařík, "Understanding data heterogeneity in the context of cyber-physical systems integration," *IEEE Trans. Ind. Informat.*, vol. 13, no. 2, pp. 660–667, Apr. 2017.

[3] X. S. Hu, J. C. Jiang, D. P. Cao, and B. Egardt, "Battery health prognosis for electric vehicles using sample entropy and sparse Bayesian predictive modeling," *IEEE Trans. Ind. Electron.*, vol. 63, no. 4, pp. 2645–2656, Apr. 2016.

[4] M. Z. A. Bhuiyan, J. Wu, W. G. J., and J. Cao, "Sensing and decision making in cyber-physical systems: The case of structural event monitoring," *IEEE Trans. Ind. Informat.*, vol. 12, no. 6, pp. 2103–2114, Dec. 2016.

[5] X. S. Hu, C. F. Zou, C. P. Zhang, and Y. Li, "Technological development in batteries: A survey in principal roles, types, and management needs," *IEEE Power Energy Mag.*, vol. 15, no. 5, pp. 20–31, Sep./Oct. 2017.

[6] M. Martínez-García, Y. Zhang, and T. Gordon, "Modelling lane keeping by a hybrid open-closed loop pulse control scheme," *IEEE Trans. Ind. Informat.*, vol. 12, no. 6, pp. 2256–2265, Dec. 2016.

[7] A. Christensen *et al.*, "Key considerations in the development of driving automation systems," in *Proc. 24th Enhanced Safety Veh. Conf.*, 2015, pp. 1–14.

[8] X. Na and D. J. Cole, "Application of open-loop stackelberg equilibrium to modeling a driver's interaction with vehicle active steering control in obstacle avoidance," *IEEE Trans. Human-Mach. Syst.*, vol. 47, no. 5, pp. 673–685, Oct. 2017.

[9] U. Rosolia, S. D. Bruyne, and A. G. Alleyne, "Autonomous vehicle control: A nonconvex approach for obstacle avoidance," *IEEE Trans. Control Syst. Technol.*, vol. 25, no. 2, pp. 469–484, Mar. 2017.

[10] C. Lv, Y. H. Liu, X. S. Hu, H. Y. Guo, D. P. Cao, and F.-Y. Wang, "Simultaneous observation of hybird states for cyber-physical systems: a case study of electric vehicle powertrain," *IEEE Trans. Cybern.*, to be published.

[11] D. González, P. Joshué, V. Milanés, and F. Nashashibi, "A review of motion planning techniques for automated vehicles," *IEEE Trans. Intell. Transport. Syst.*, vol. 17, no. 4, pp. 1135–1145, Apr. 2016.

[12] J. Guo, P. Hu, and R. Wang, "Nonlinear coordinated steering and braking control of vision-based autonomous vehicles in emergency obstacle avoidance," *IEEE Trans. Intell. Transport. Syst.*, vol. 17, no. 11, pp. 3230–3240, Nov. 2016.

[13] H. Li, S. X. Yang, and M. L. Seto, "Neural-network-based path planning for a multirobot system with moving obstacles," *IEEE Trans. Syst., Man, Cybern. C, Appl. Rev.*, vol. 39, no. 4, pp. 410–419, Jul. 2009.

[14] N. Wang, S. Lv, M. J. Er, and W.-H. Chen, "Fast and accurate trajectory tracking control of an autonomous surface vehicle with unmodeled dynamics and disturbances," *IEEE Trans. Intell. Veh.*, vol. 1, no. 3, pp. 230–243, Sep. 2016.

[15] H. Chen, *Model Predictive Control*. Beijing, China: Science press, 2013.

[16] H. Y. Guo, F. Liu, R. Yu, Z. P. Sun, and H. Chen, "Regional path moving horizon tracking controller design for autonomous ground vehicles," *Sci. China Inf. Sci.*, vol. 60, no. 1, p. 013201, Mar. 2017.

[17] H. Y. Guo, J. Liu, D. P. Cao, H. Chen, R. Yu, and C. Lv, "Dual-envelop-oriented moving horizon path tracking control for fully automated vehicles," *Mechatronics*, to be published.

[18] H. Dahmani, M. Chadli, A. Rabhi, and A. Hajjaji, "Road curvature estimation for vehicle lane departure detection using a robust Takagia-Sugeno fuzzy observer," *Veh. Syst. Dyn.*, vol. 51, no. 5, pp. 581–599, 2013.

[19] T. D. Gillespie, *Fundamentals of Vehicle Dynamics*. New York, NY, USA: SAE Press, 1992.

[20] J. H. Kim and J. B. Song, "Control logic for an electric power steering system using assist motor," *Mechatronics*, vol. 12, pp. 447–459, Mar. 2002.

[21] Mobileye, *Quick Reference Guide*, 2008. [Online]. Available: www.mobileye.com

[22] H. Y. Guo, F. Liu, F. Xu, H. Chen, and Y. Ji, "Nonlinear model predictive lateral stability control of active chassis for intelligent vehicles and its FPGA implementation," *IEEE Trans. Syst., Man, Cybern., Syst.*, to be published.

[23] A. L. Burgett, R. J. Carter, and Miller, "A collision warning algorithm rear-ends collisions," in *Proc. Int. Tech. Conf. Enhanced Safety Veh.*, 1998, pp. 566–587.
[24] Y. F. Cong, *Motion Planning and Control for Autonomous Vehicle Driving on Motorways*. Jilin, China: Jilin Univ., 2011.
[25] D. Pan and Y. P. Zheng, "Velocity difference control based on dynamic tracking of safe following distance in the process of vehicle following," *IET Intell. Transport Syst.*, vol. 8, no. 3, pp. 232–243, 2014.
[26] Q. Zhang, L. Lapierre, and X. B. Xiang, "Distributed control of coordinated path tracking for networked nonholonomic mobile vehicles," *IEEE Trans. Ind. Informat.*, vol. 9, no. 1, pp. 472–484, Feb. 2013.
[27] C. Shen, Y. Shi, and B. Buckham, "Integrated path planning and tracking control of an AUV: A unified receding horizon optimization approach," *IEEE/ASME Trans. Mechatronics*, vol. 22, no. 3, pp. 1163–1173, Jun. 2017.
[28] M. C. B., J. Y. Cao and Y. Qiao, "Polynomial-method-based design of low-order controllers for two-mass systems," *IEEE Trans. Ind. Electron.*, vol. 60, no. 3, pp. 969–978, Mar. 2013.
[29] K. Han, M. Lee, E. Choi, and S. B. Choi, "Adaptive scheme for the real-time estimation of tire-road friction coefficient and vehicle velocity," *IEEE Trans. Mechatronics*, vol. 22, no. 4, pp. 1508–1518, Aug. 2017.

Hongyan Guo (M'17) received the PH.D. degree in control theory and control engineering from the Jilin University, Changchun, China, in 2010.

She joined the Jilin University, in 2011, where from 2014, she is an Associate Professor with the Department of Control Science and Engineering. In 2017, she is a Visiting Scholar with Cranfield University, Cranfield, U.K. Her current research interests include path tracking and stability control of autonomous vehicles and vehicle states estimation.

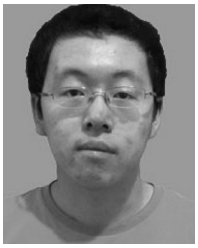

Chen Shen received the B.Sc. degree in automation from the Jilin University, Changchun, China, in 2016, where he is currently working toward the M.Sc. degree with the Department of Control Engineering and Control Theory.

His current research interests include active safety and autonomous driving, particularly path planning and path tracking for autonomous vehicle.

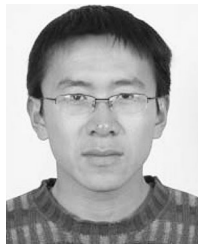

Hui Zhang (M'15–SM'17) received the B.Sc. degree in mechanical design manufacturing and automation from the Harbin Institute of Technology at Weihai, Weihai, China, in 2006, the M.Sc. degree in automotive engineering from Jilin University, Changchun, China, in 2008, and the Ph.D. degree in mechanical engineering from the University of Victoria, Victoria, BC, Canada, in 2012.

He is with the School of Transportation Science and Engineering, Beihang University, Beijing, China. His research interests include diesel engine aftertreatment systems, vehicle dynamics and control, mechatronics, robust control and filtering, networked control systems, and multiagent systems. He is an author / co-author of more than 80 peer-reviewed papers on journals and conference proceedings.

Hong Chen (M'02–SM'12) received the Ph.D. degree in system dynamics and control engineering from the University of Stuttgart, Stuttgart, Germany, in 1997.

She joined the Jilin University of Technology, Changchun, China, in 1986, where she became an Associate Professor in 1998 and has been a Professor since 1999. Her current research interests include model predictive control, optimal and robust control, and applications in process engineering and mechatronic systems.

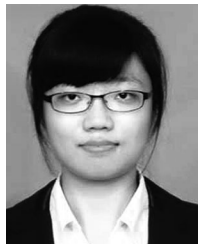

Rui Jia received the M. Sc. degree in control theory and control engineering from the Jilin University, Changchun, China, in 2014.

She is currently an Engineer with Weichai Power Co. Ltd, Weifang, China. She is currently researching on software development of Engine Control Unit, particularly the control of fuel system and software framework design.